Fe_3O_4-polyaniline nanofibers synthesis in non-ionic surfactant based swollen liquid crystals

Shivkumar Y. Patil[1], Pramod P. Mahulikar[1], Sandeep J. Pawar[1], Vishwanath. S. Zope[2*]

1 School of Chemical Sciences, North Maharashtra University, Jalgaon, 425001 Maharashtra, India.

2 Department of Chemistry, Moolji Jaitha College, Jalgaon 425001 Maharashtra, India

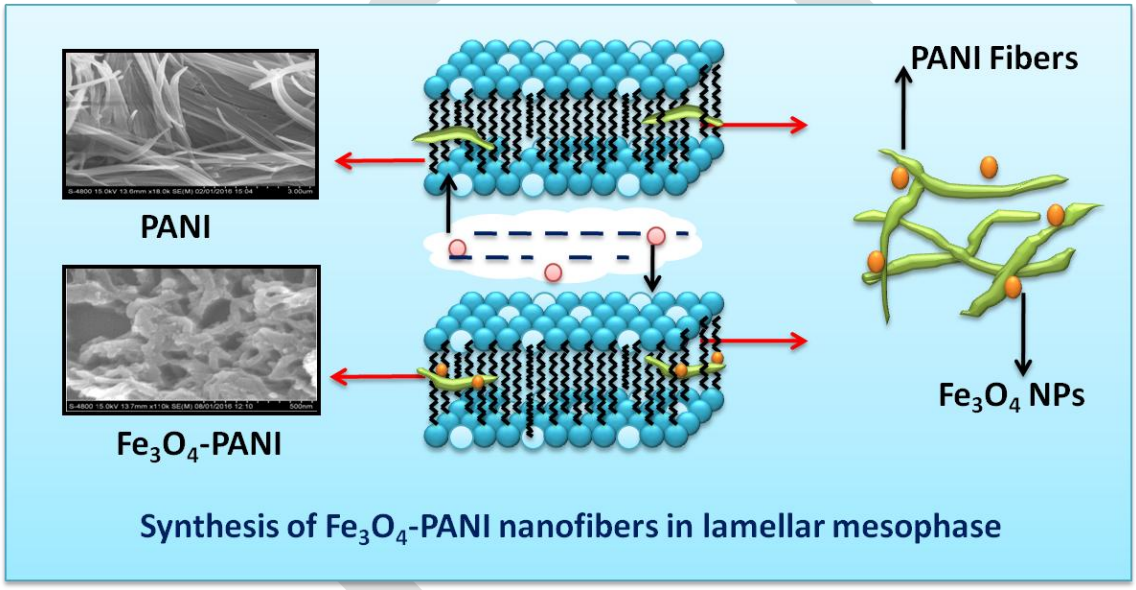

Graphical abstract

Abstract

Polyaniline (PANI) and Fe_3O_4-PANI composite nanofibers were synthesized for the first time using non-ionic surfactant based "soft templates". Prepared lamellar mesophase with PANI and nanocomposites was confined by using polarized optical microscope. The synthesized nanocomposite showed PANI fibre diameters ranging from 70-300 nm as observed in FESEM. For the electrochemical measurements PANI and Fe_3O_4-PANI nanocomposite material was coated on stainless steel plates and 1M H_2SO_4 was used as a electrolyte. The capacitance measured by CV showed pseudocapacitance behaviour of PANI and Fe_3O_4-PANI and the nano Fe_3O_4-PANI modified electrodes showed higher value of the capacitance as compared to PANI nanofibres.

Keywords: Swollen liquid crystal; magnetic nanoparticles; polyaniline nanofibers; supercapacitors.

Corresponding author:

To whom correspondence should be addressed:

Prof. Dr. V. S Zope

Department of Chemistry,

Moolji Jetha College,

Jalgaon 425 001 Maharashtra,

India

Mobile No: +91 9422224616

1. Introduction

Synthesis of nanomaterials with the controlled morphology of nanostructures is new advancement in the field of nanoscience and nanotechnology [1]. Surfactant based swollen liquid crystals (SLCs) such as hexagonal and lamellar mesophases are structure directing templates in new synthetic way for material chemistry [2]. The "hard" template constitute solid like mesoporous silica which uses harsh chemical treatments after post synthesis. On the other hand, use of "soft" templates is easy as well as convenient for separation of motifs like polymers and surfactants [3]. Polyaniline (PANI) is one of the most important conducting polymer (CP) because of high conductivity, ease to synthesis, low cost and good environmental stability [4]. Potential application of PANI derivatives were reported in the field of batteries, capacitors, fuel cells and gas sensing devices [5-7]. It can be synthesized via chemical, electrochemical and template assisted methods [8]. Nanocomposites of CPs with inorganic materials such as metal oxides, carbon based nanostructures have been thoroughly utilized in various applications such as electrochemical sensors, energy storage and catalysis [9-10]. Synthesis of Fe_3O_4 nanoparticles are emerged as mechanical, electromagnetic shielding materials and catalyst for degradation of environmental pollutants [11].

Additionally, Fe_3O_4 nanoparticles based nanocomposites are synthesized by using variety of methods such as chemical, blending with co-precipitation, picker emulsion and interfacial polymerization to produce core-shell nanostructures [12-13]. Literature reported hitherto revealed that the nanocomposites of Fe_3O_4 with PANI were used for chemical oxidation polymerization for microwave absorbents and electromagnetic shielding coatings [12, 14].

Recently, synthesis of organic conducting polymers and metal nanoparticles in hexagonal swollen liquid crystals (SLCs) has been successfully used for the chemical polymerization of 1-D PEDOT, PANI and core shell structures of Au-PANI [3, 15-16]. SLCs

are formed by using quaternary system of oil, water, surfactant and co-surfactant and they can be used as hexagonal SLCs as soft templates for synthesis of Pt and Pd nanostructures [17-18].

In the present study, we have reported the first time nanoscale synthesis of 1-D PANI and Fe_3O_4-PANI nanostructures. We have designed nanofibers of these two motifs in swollen lamellar mesophase based on non-ionic surfactant Triton X-100. *In-situ* chemical oxidation polymerization of PANI and Fe_3O_4-PANI nanocomposite in swollen lamellar mesophase was performed using ammonium persulfate (APS) as an oxidant.

2. Experimental

2.1 *Materials*

The non-ionic surfactant (Triton X-100) was procured from fisher-scientific and aniline (99.5%), ammonium persulfate (98%), cyclohexane (99.8%) and 1-pentanol (98%) were purchased from Merck.

2.2 *Synthesis of Polyaniline (PANI) in lamellar mesophase*

2.4 g of non-ionic surfactant Triton X-100 was dissolved in 2 mL of 0.1 M HCl solution at 35 ^{o}C. After complete dissolution of the surfactant, 3.3 mL of cyclohexane (oil) containing 4 mM of aniline monomer was added to the surfcatant mixture with vigorous vortexing. 1-Pentanol (co-surfactant) was then added to the mixture and strongly vortexed for a few minutes [19]. This resulted into perfectly transparent and unstable gel that is a lamellar mesophase. Then 8 mM of APS initiator was added to this mixture with continuous vortexing, to afford a dark green colored of PANI fiber in mesophase. **(Scheme 1)**

2.3 *Synthesis of Fe_3O_4-PANI in lamellar mesophase*

Synthesis of Fe_3O_4 nanoparticles was achieved according to reported method [20]. Aqueous 0.1 M HCl (2 ml) with magnetic nanoparticles was sonicated and 2.4 g of non-ionic surfactant was added in it. After complete dissolution of the surfactant, 3.3 mL of cyclohexane (oil) containing 4 mM of aniline monomer was added to the mixture with vigorous vortexing (monomer:Fe_3O_4, 4:1). Consequently 1-pentanol (co-surfactant) was added to this mixture and strongly vortexed for a few minutes. This leads to a perfectly unstable gel: a lamellar mesophase. Then APS as initiator was added this phase with continuous vortex resulting into subsequent color change. (Fig. S1 supporting information)

The lamellar mesophase was optimized by the ratio of aniline: APS (2:1) for synthesis of PANI nanofibers and its nanocomposites in soft templates. In order to characterize the synthesized material in lamellar mesophase, the mesophase was destabilized by iso-propanol and double distilled water centrifugation cycle. The dried samples were analyzed by FTIR, FESEM, XRD, TGA, UV-Visible spectrophotometer and electrochemical measurements.

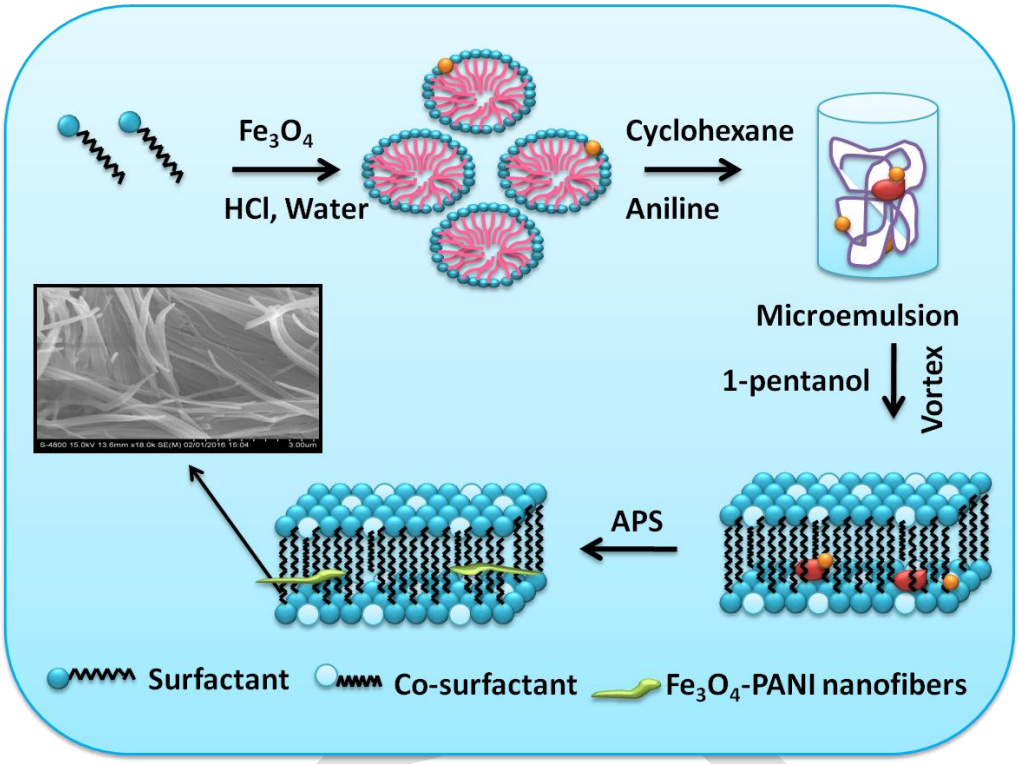

Scheme 1. Schematic representation of PANI and nanocomposites synthesized in non-ionic surfactant assisted soft templates.

2.4 *Charecterization*

Swollen liquid crystals (SLCs) (before and after polymerization) were characterized by polarized optical microscope (Leica DM 750 P). FESEM observations were performed with S-4800 Hitachi, USA at an accelerating voltage of 30 kV. FTIR spectra of PANI nanofibers were analyzed by Alpha instrument from Bruker in the range 400 to 4000 cm^{-1}. XRD patterns of the samples were conducted with D8 Advance Bruker Ltd. Germany Diffractometer using Cu Kα radiation. TGA was recorded using Perkin Elmer 4000 TG Analyzer. UV-Visible spectra were recorded by Agilent Technologies Carry 60 UV-Vis spectrophotometer.

2.5 *Electrochemical Measurements*

Cyclic voltammetry measurements were performed with an Autolab PGSTAT-30 electrochemical workstation (Metrohm, India), using three-electrode system. For modifications of SS plates, 85 % of synthesized nanocomposite Fe_3O_4-PANI and PANI, 5 % PVDF and 10 % carbon black were dissolved in N-methyl pyrrolidone (NMP) solvent. The modified electrodes were prepared by dip coating of prepared nanocomposites solution on polished stainless steel plates [21]. For the electrochemical measurements modified SS electrodes were used as a working, platinum wire as counter and Ag/AgCl as a reference electrodes. The CV curves were collected at different scan rates ranging from 10 to 100 mV/s with the potential range of -0.2 to 1 V. The electrochemical tests were carried out in 1 M H_2SO_4 electrolyte solution at ambient temperature.

3. Results and Discussion

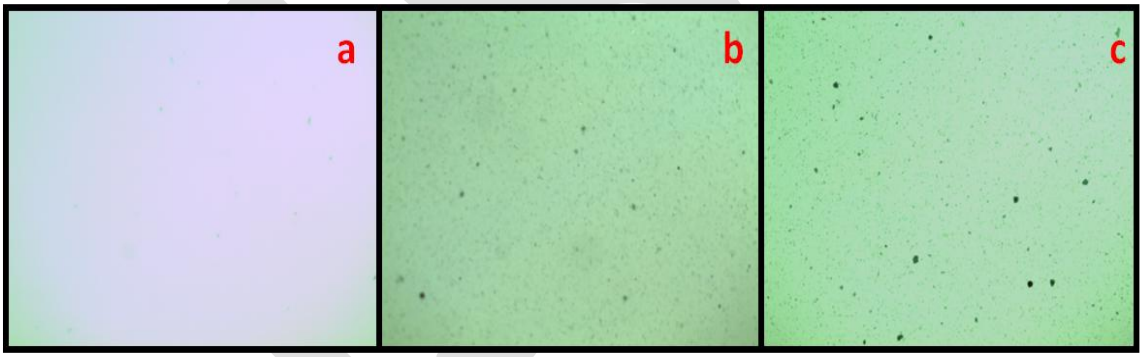

Fig. 1. Polarized optical microscope images of (a) lamellar mesophase, (b) synthesized PANI in mesophase and (c) synthesized Fe_3O_4-PANI in mesophase using Triton X-100.

Polarized optical microscope image of lamellar mesophase was found to be clear as shown in Fig. 1a. Small dark blue colored particles were observed in Fig. 1b that depicted the successful synthesis of PANI in mesophase. Similarly, Fig. 1c showed the Fe_3O_4 doped nanocomposites in mesophase. As reported by Ghosh et.al. [16] Synthesized PANI and

Fe_3O_4-PANI nanocomposites in mesophase for dark blue colored particles are entrapped into the lamellar mesophases are believable and are more reliable.

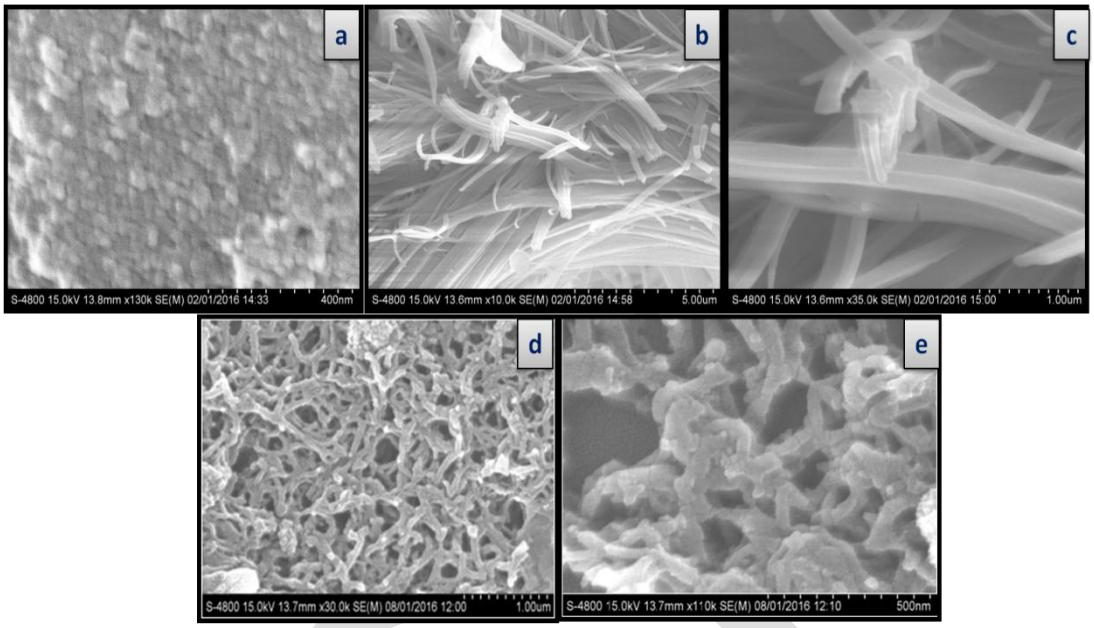

Fig. 2. FESEM images of (a) Fe_3O_4, (b, c) PANI and (d, e) Fe_3O_4-PANI.

The FESEM study demonstrated spherical form of Fe_3O_4 nanoparticles with an average diameter of 40 nm as shown in Fig. 2 a. Synthesized PANI using Triton X-100 assisted template showed longer, uniform and smooth surfaces of the PANI nanofibres with an average diameter of 200-300 nm (Fig. 2b and c). Fe_3O_4 nanoparticles doped on the surfaces of PANI showed Fe_3O_4 nanoparticles decorated nanofibers with an average diameter of 100-130 nm. (Fig. 2d & 2e)

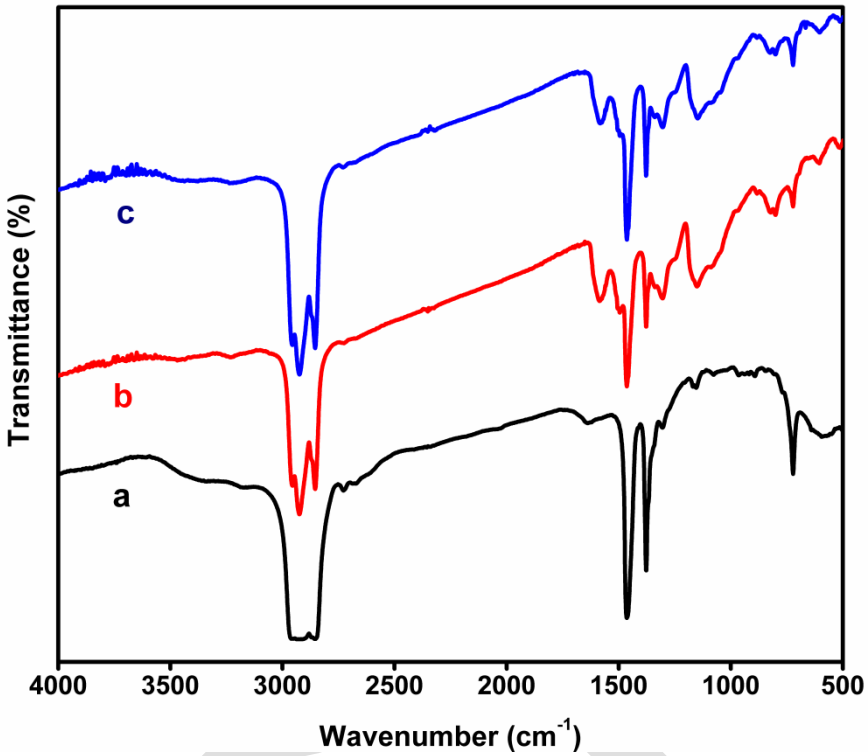

Fig. 3.FTIR spectra of (a) Fe_3O_4, (b) PANI and (c) Fe_3O_4-PANI.

The FTIR spectra of Fe_3O_4, PANI and PANI-Fe_3O_4 composite are shown in Fig. 3. In the IR spectrum Fe_3O_4 (Fig. 3a), the peak at 577 cm^{-1} was attributed to the characteristic band of Fe-O vibration. The IR spectrum of PANI (Fig. 3b), the band at 1301 cm^{-1} was corresponds to the stretching vibration of C-N, 1147, and 821 cm^{-1} were corresponded to out of plane deformation of C-H in the 1,4-disubstituted benzene ring. In IR spectrum of Fe_3O_4-PANI nanocomposites (Fig. 3c) the characteristic band at 1582 cm^{-1} was due to the C=C stretching deformation of quinoid and benzenoid ring of PANI. The IR spectra confirmed that the Fe_3O_4 nanoparticles were decorated on the surface of PANI nanofibres.

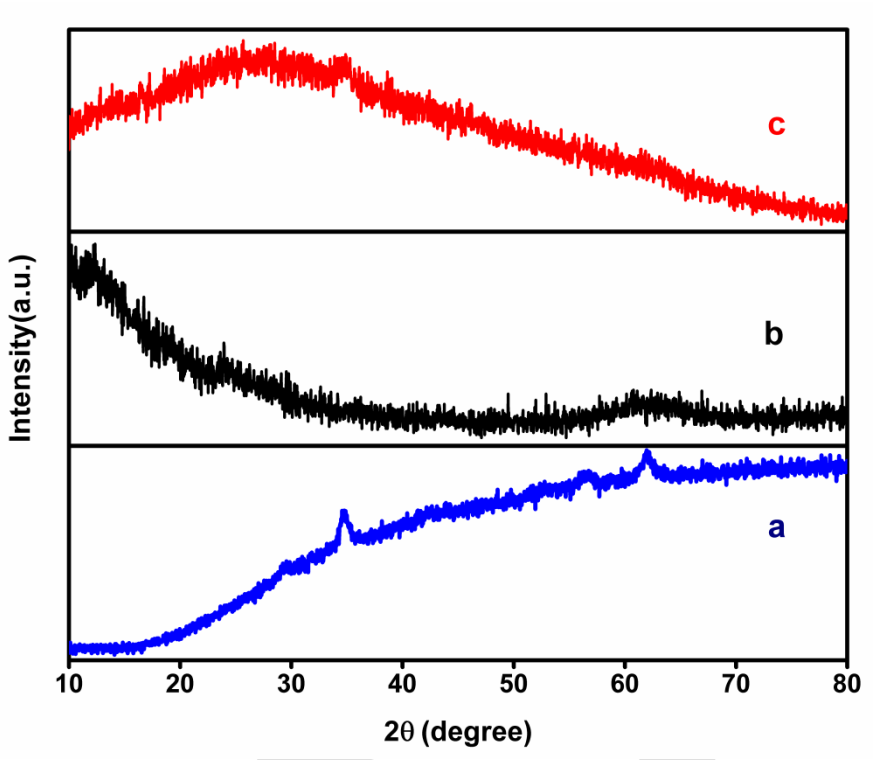

Fig. 4. XRD of (a) Fe_3O_4, (b) PANI and (c) Fe_3O_4-PANI.

A comparative x-ray diffraction pattern of pristine Fe_3O_4, PANI and Fe_3O_4-PANI nanocomposite are depicted in Fig. 4. In case of Fe_3O_4 nanoparticles, Bragg's peaks at 29.37, 34.78, 42.32, 52.85, 56.52 and 62.15 are ascribed to (220), (311), (400), (422), (511) and (440) planes respectively, which shows that the Fe_3O_4 nanoparticles are with cubic spinel structure. For PANI (Fig. 4b) 2θ = 19.47 and 24.04 were due to the periodicity that is parallel and perpendicular to the molecular chains of PANI and its polycrystalline in nature. For composites material (Fig. 4c), a broad hump like shape was observed however, Bragg's peak at 34.78^o confirmed the successful grafting of Fe_3O_4 nanoparticles on the surface of PANI nanofibres.

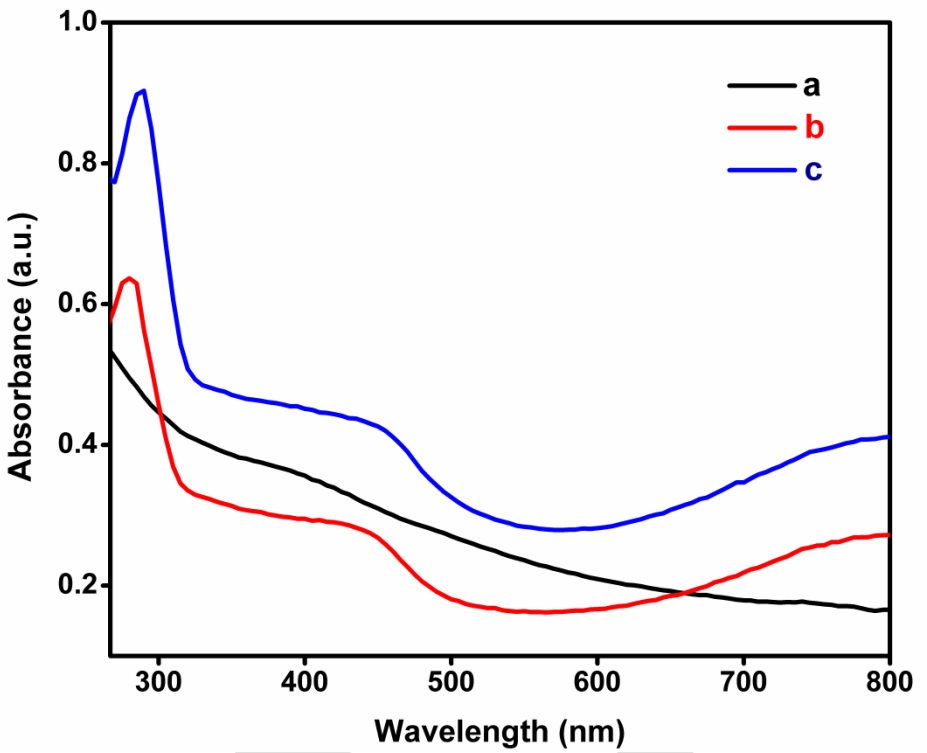

Fig. 5. UV-Visible spectra of (a) Fe_3O_4, (b) PANI and (c) Fe_3O_4-PANI.

No significant absorption peaks were observed for in Fe_3O_4 nanoparticles (Fig. 5a). PANI-Fe_3O_4 exhibited two characteristic bands at 280 and 443 nm, which could be attributed to the π-π* transition of the benzenoid ring and the benzenoid-quinoid excitonic transition, respectively (Fig. 5c).

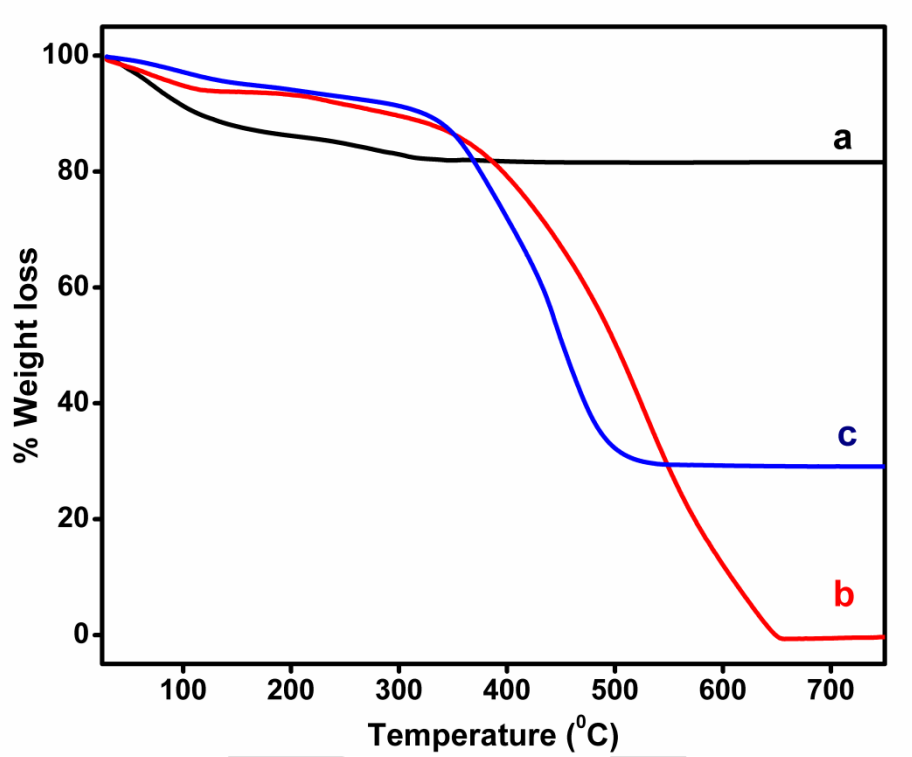

Fig. 6. TGA spectra of (a) Fe_3O_4, (b) PANI and (c) Fe_3O_4-PANI.

In thermal analysis, Fe_3O_4 nanoparticles showed weight loss above 200 ^{0}C was because of the oxidation of Fe_3O_4 to γ-Fe_3O_4 and further weight loss of 19% in the range of 300 to 750 ^{0}C (Fig. 6a). In PANI samples two stage degradation was observed, first stage at 130 ^{0}C due to water or moistures and second stage complete degradation of backbone of polymer chain (Fig. 6b). Lastly, Fe_3O_4 doped composites first weight loss similar water molecules eliminate and second step 130 to 750 ^{0}C weight loss is 30 % due to the incorporate Fe_3O_4 nanoparticles (Inorganic residue) on the surface of polymeric nanofibers (Fig. 6c). This is confined that the thermal stability of nanocomposites is enhanced than the PANI nanofibers.

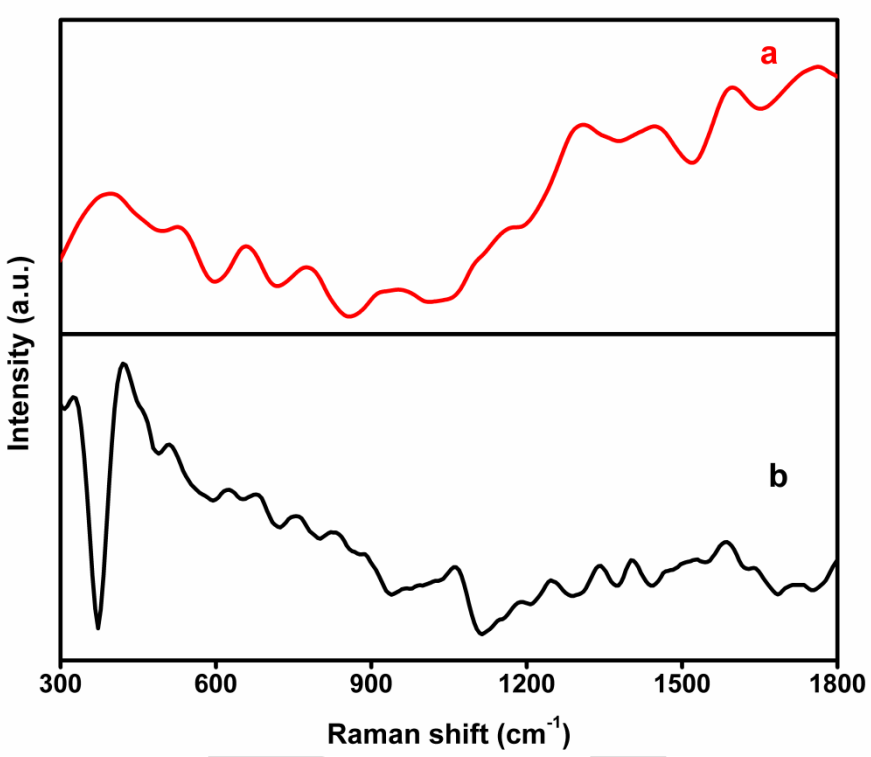

Fig.7. Raman spectra of (a) Fe_3O_4 and (b) Fe_3O_4-PANI.

In Raman spectrum of Fe_3O_4 nanoparticles (Fig. 7a), the peaks at 660 and 536 cm^{-1} were ascribed to the A1g and T2g modes of Fe_3O_4 nanoparticles. However in the spectrum of Fe_3O_4-PANI nanocomposites (Fig. 7b), the additional peaks at 1176, 1336, 1467 and 1584 cm^{-1} were corresponded to the C-H bending of quinoid/benzenoid ring, C-N stretching, C=N stretching of quinoid ring and C-N stretching of benzenoid ring respectively, that confirmed the grafting.

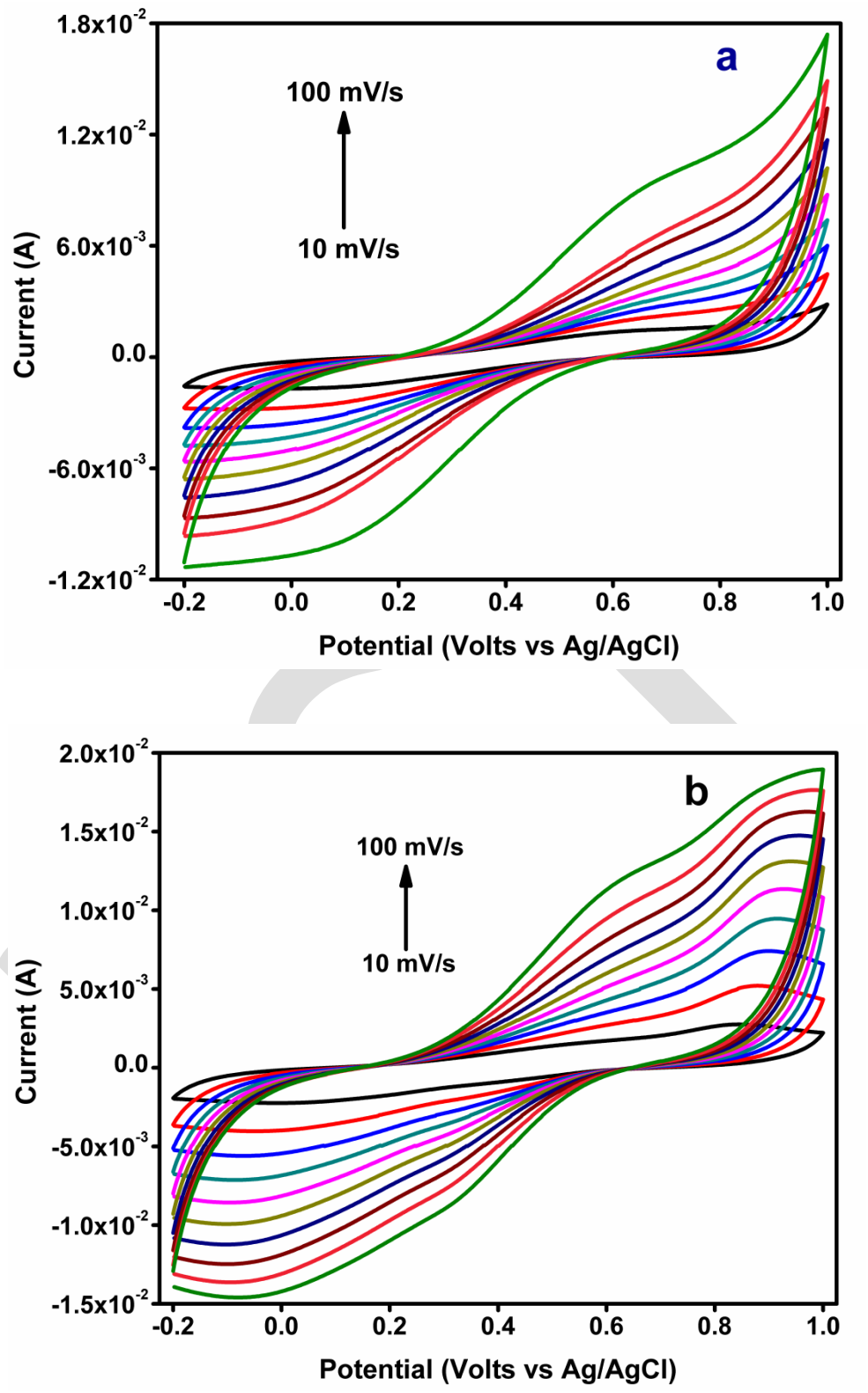

Fig. 8. Cyclic voltammetry of (a) PANI and (b) Fe_3O_4-PANI nanocomposites at 10 to 100 mV/s scan rates the potential range -0.2 to 1 V in 1M H_2SO_4.

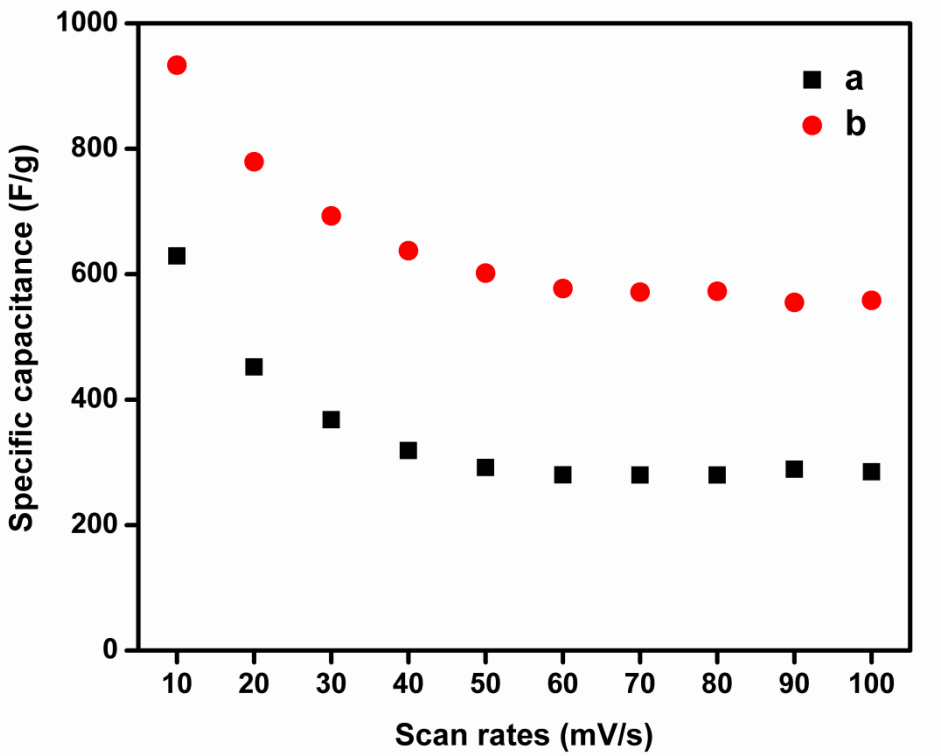

Fig. 9. Specific capacitance of (a) PANI and (b) Fe_3O_4-PANI nanofibers from CV vs. scan rates.

Cyclic voltammetry (CV) was used to explore electrochemical properties of PANI and Fe_3O_4-PANI at 10, 20, 30, 40, 50, 60, 70, 80, 90, 100 mV/s scan rates in 1M H_2SO_4 aqueous solution with the potential range of -0.2 to 1 V vs. Ag/AgCl. The CV curves of PANI nanofibers depicted two pairs of redox peaks (Fig. 8a), which is due to the pseudocapacitance behaviour. The first pair of redox peak was located at low potential corresponded to the redox transition of PANI from leucoemeraldine to emeraldine state and the redox peak located at high potential was attributed to the transformation from emeraldine to pernigraniline state [22]. The Fe_3O_4-PANI nanocomposite showed increasing CV loops compared to PANI its good sign for the capacitance (Fig. 8b). The increasing scan rates with increasing current clearly indicated that the composites material and PANI nanofibers electrodes have good rate stability [23].

Specific capacitance of the electrode materials was calculated by using following equation from CV curves,

$$C = \int Idv/2mvV$$

Where, C is specific capacitance of the mass of electroactive materials (F/g), I is the response current (A), V is potential (V), v is potential scan rate (V/s) and m is the mass of active electrode materials (g). Specific capacitance for PANI was found to be 629.16 and that of Fe_3O_4-PANI was 933.33 F/g at 10 mV/s scan rate (Fig. 9). The study clearly exhibited that nanocomposites material capacitance was enhanced in comparison with the PANI nanofibers, due to the synergistic effect between Fe_3O_4 nanoparticles and PANI nanofibers.

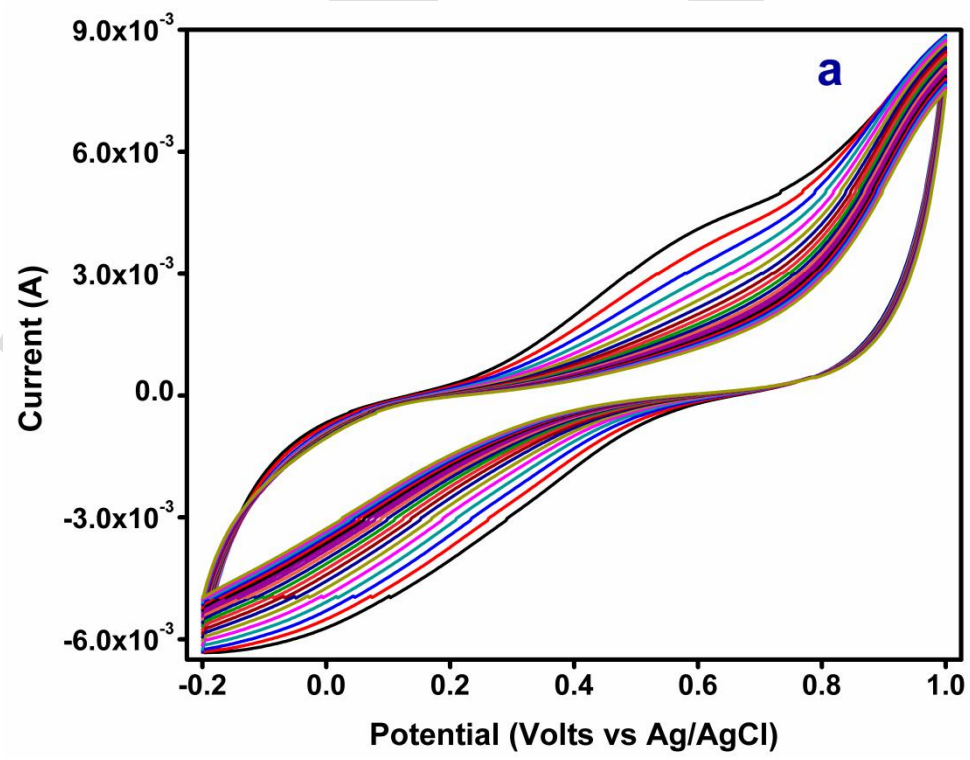

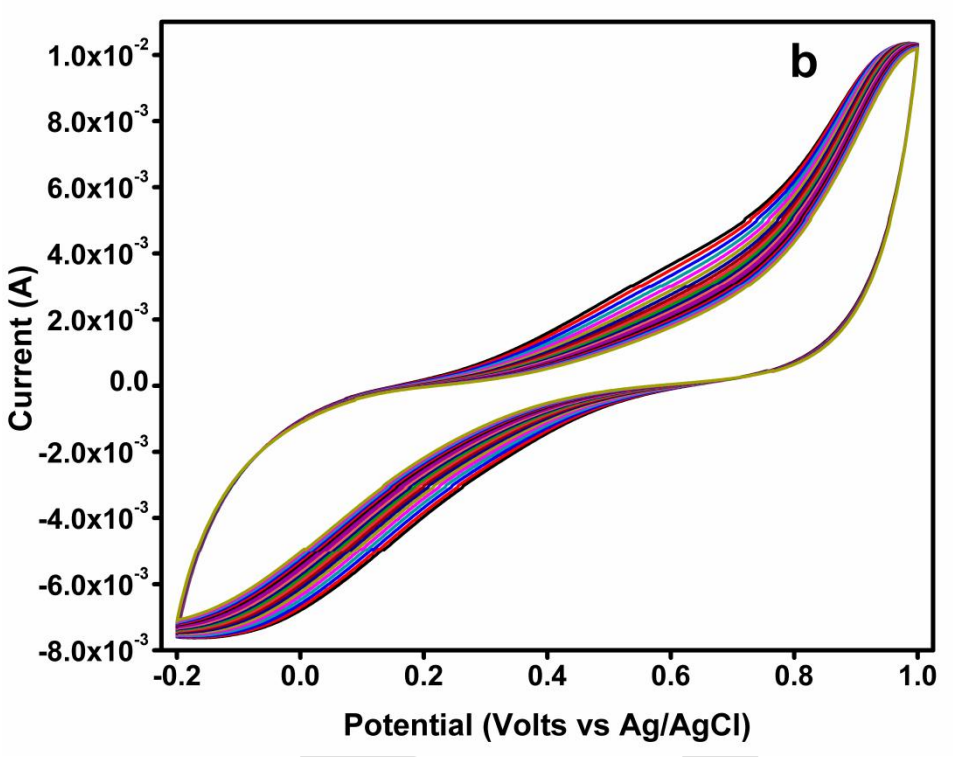

Fig. 10.CV curves of (a) PANI and (b) Fe_3O_4-PANI at 50 mV/s scan rate.

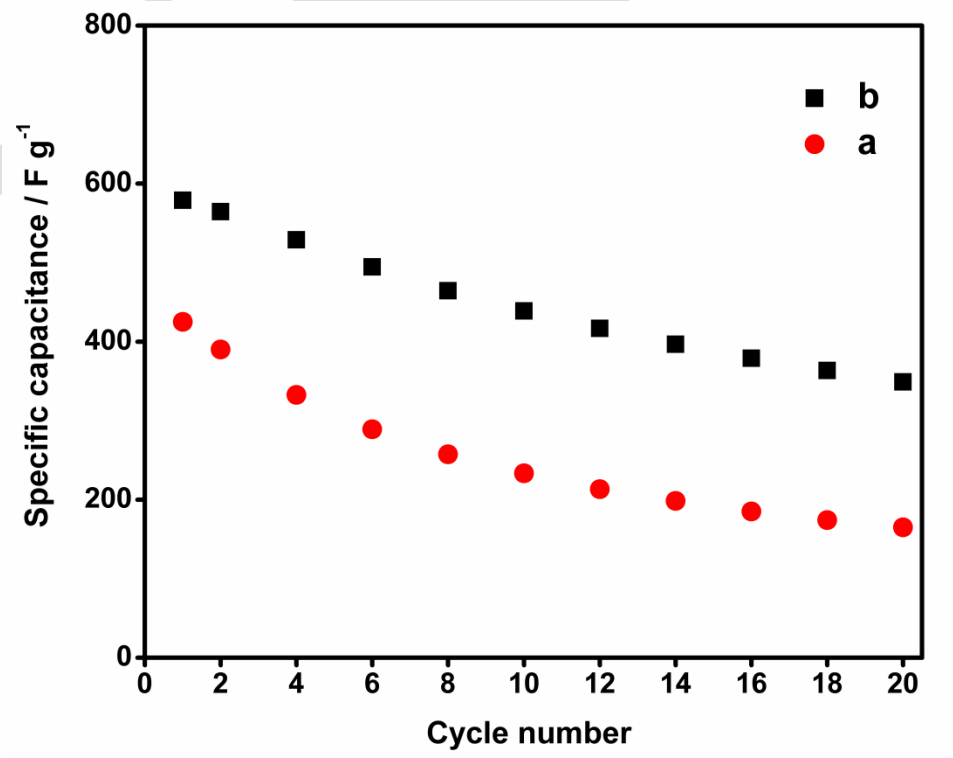

Fig. 11. Specific capacitance of PANI and Fe_3O_4-PANI sweep potential at 50 mV/s.

Fig. 10 shows the cyclic stability of PANI nanofibers and PANI-Fe_3O_4-PANI at the sweep rate of 50 mV/s for 20 cycles. Specific capacitance value was linearly decreasing for 10 cycles and subsequently the specific capacitance remained nearly constant (Fig. 11b). The specific capacitance of PANI nanofibers was 425 F/g in the first cycle and 165 F/g in the 20 cycles (Fig. 11a) clearly indicated that the Fe_3O_4 doped nanocomposites have high stability of the electrode material than PANI nanofibers for long cyclic life.

4. Conclusion

In the present work, we successfully synthesised the PANI and Fe_3O_4-PANI composite nanofibers using SLCs as soft templates. The synthesised Fe_3O_4-PANI nanocomposites were found to be concretely confinements due to the strong interaction between Fe_3O_4 nanoparticles on the surface of PANI nanofibers. The study revealed that conductive material PANI and Fe_3O_4-PANI nanofibers have plausible application as supercapacitor as they showed significant capacitance values of 629 F/g and 933 F/g, respectively.

Supplementary Information (SI)

Digital camera photographs are shown in supplementary information.

Acknowledgement

SYP grateful to DST-INSPIRE (IF-120468), New Delhi for providing financial support.

References

1. G. Surendran, L. Ramos, B. Pansu, E. Prouzet, P. Beaunier, F. Audonnet, H. Remita, Chem. Mater. 19 (2007) 5045.
2. S. Dutt, P. F. Siril, J. App. Poly. Sci. 131 (2014) 40801.
3. S. Dutt, P. F. Siril, Mat. Lett. 124 2014 50.
4. M. Nandi, R. Gangopadhyay, A. Bhaumik, Micro and Meso. Mate. 109 (2008) 239.
5. J. Huang, S. Virji, B. H. Weiller, R. B Kaner, J. Am. Chem. Soc. 125 (2003) 314.
6. J. Huang, R. B. Kaner, J. Am. Chem. Soc. 126 (2004) 851.
7. S. Virji, J. Huang, R. B. Kaner, B. H. Weiller, Nano lett. 4 (2004) 491.
8. Y. Wang, Z. Liu, B. Han, Z. Sun, Y. Huang, G. Yang, Langmuir. 21 (2005) 833
9. Y. Wang, L. Gai, W. Ma, H. Jiang, X. Peng, L. Zhao, Ind. & Eng. Chem. Res. 54 (2015) 2279.
10. L. Li, A. R. O. Raji, H. Fei, Y. Yang, E. L. Samuel, J. M. Tour, ACS Appl. Mate. & Inter. 5 (2013) 6622.
11. T. Yao, T. Cui, H. Wang, L. Xu, F. Cui, J. Wu Nanoscale. 6 (2014) 7666.
12. L. Gai, X. Han, Y. Hou, J. Chen, H. Jiang, X. Chen, Dalt. Trans. 42 (2013) 1820.
13. Q. Xiao, X. Tan, L. Ji, J. Xue, Synth Metals. 157 (2007) 784.
14. C. Cui, Y. Du, T. Li, X. Zheng, X. Wang, X. Han, P. Xu, J. Phy. Chem. B. 116 (2012) 9523.
15. S. Ghosh, H. Remita, L. Ramos, A. Dazzi, A. Deniset-Besseau, P. Beaunier, G. Fabrice, A. Pierre-Henri, B. Francois, S. Remita, New J. Chem. 38 (2014) 1106.
16. S. Dutt, P. F. Siril, V. Sharma, S. Periasamy, New J. Chem. 39 (2015) 902.
17. A. M. Kalekar, K. K. K. Sharma, A. Lehoux, F. Audonnet, H. Remita, A. Saha, G. K. Sharma, Langmuir. 29 (2013) 11431.

18. A. M. Kalekar, K. K. Sharma, N. M. Luwang, G. K. Sharma, RSC Advances (2016) DOI: 10.1039/C5RA23138H.
19. G. Surendran, M. S. Tokumoto, E. Pena dos Santos, H. Remita, L. Ramos, P. J. Kooyman, C. V. Santilli, C. Bourgaux, P. Dieudonne, E. Prouzet, Chem. Mate., 17 (2005) 1505.
20. A. R. Mahdavian, M. A. S. Mirrahimi, Chem. Eng. J. 159 (2010) 264.
21. W.Wang, Q. Hao, W. Lei, X. Xia, X. Wang, RSC Advances, 2 (2012) 10268.
22. L. F. Chen, X. D. Zhang, H. W. Liang, M. Kong, Q. F. Guan, P. Chen, W. Zhen-Yu, S. H. Yu, ACS Nano, 6 (2012) 7092.
23. V. Gupta, N. Miura, Mate. Lett. 60 (2006) 1466.

Figure S1. Digital camera photographs of (a) lamellar mesophase in Triton X-100 in presence of 4 mM ANI (b) lamellar mesophase doped with Fe_3O_4 nanoparticles. (c) The dark green color was observed which indicate polymerization of ANI. (d) Synthesis of Fe_3O_4-PANI nanocomposites in swollen liquid crystal.

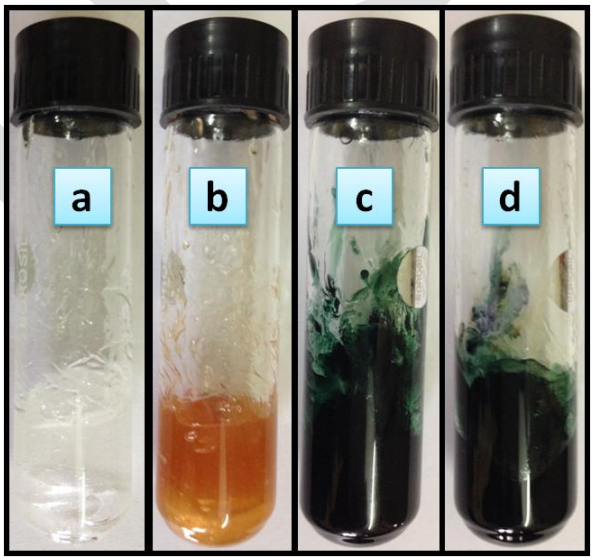

S1